Stem Cell Research & Therapy

RESEARCH

Open Access

Human umbilical cord mesenchymal stem cell therapy for atopic dermatitis through inhibition of neutrophil chemotaxis

Jinjin Shao[1†], Zhiqi Xie[2†], Zhichao Ye[1], Guoyu Chen[1], Yiru Wang[5], Lili Zhang[1], Fang Liu[1], Siming Zhang[1], Xiaobo Lin[1], Jiahong Wang[1], Ying Chen[1], Yunxiang Chen[1], Xin Pan[3], Feifei Wu[3], Ruolang Pan[3*], Jinfeng Liang[4*] and Lijiang Zhang[1,6*]

Abstract

Background Atopic dermatitis (AD) management is significantly challenging due to the high prevalence, chronicity, and recurrent nature of the disease, and limited options for its treatment. Human umbilical cord mesenchymal stem cells (hUC-MSCs) exhibit potential effects against AD; however, the mechanisms underlying these effects remain largely unexplored.

Methods AD mouse models were established using 1-chloro-2,4-dinitrobenzene (DNCB) and ovalbumin (OVA). The therapeutic effects of subcutaneously administered hUC-MSCs and their conditioned medium (hUC-MSC-CM) were evaluated through histopathology, western blotting, PCR, ELISA, and flow cytometry. Mechanistic studies included RNA sequencing, cytokine arrays, and exosome characterization.

Results Both hUC-MSCs and hUC-MSC-CM significantly alleviated AD-like symptoms, including erythema, epidermal thickening, and inflammatory cell infiltration in DNCB- and OVA-induced models. There was a decrease in serum IgE levels and histological analyses confirmed attenuated skin damage in these models. Moreover, neither hUC-MSCs nor hUC-MSC-CM induced weight loss. Mechanistically, hUC-MSC-CM suppressed neutrophil migration in the skin and inhibited keratinocyte-derived chemokine (e.g., CCL5 and CXCL11) secretion. Additionally, hUC-MSC-derived exosomes reduced chemokine production in keratinocytes, mediated by the STAT3 signaling pathway.

Conclusions This study demonstrated that hUC-MSCs and hUC-MSC-CM ameliorate AD-like symptoms, possibly through exosome-dependent suppression of the STAT3 signaling pathway and chemokine expression. Furthermore, hUC-MSC-CM serves as a cell-free alternative to whole-cell therapy, with comparable efficacy, offering novel mechanistic insights and a potential translational strategy for AD treatment.

Keywords Atopic dermatitis, Human umbilical cord mesenchymal stem cells, Keratinocytes, Neutrophil chemotaxis, JAK-STAT signaling pathway

†Jinjin Shao and Zhiqi Xie have contributed equally to this work.

*Correspondence:
Ruolang Pan
panrl@zju.edu.cn
Jinfeng Liang
liangwind@sohu.com
Lijiang Zhang
zhanglj127@163.com
Full list of author information is available at the end of the article

Background

Atopic dermatitis (AD) is a chronic inflammatory skin condition, often described as an "immortal cancer" owing to its persistent nature and the challenges associated with its treatment [1]. Overall, 223 million people are affected by AD worldwide, with a significant incidence of 30% among children. Moreover, 40% of patients experience severe symptoms, such as persistent rash, intense itching, sleep disruption, and comorbidities, including asthma, depression, and anxiety [2, 3]. AD is the most debilitating non-fatal skin ailment, imposing significant psychological and financial strain on patients and their families [4]. Its complex pathogenesis involves genetic predisposition, environmental triggers, impaired skin function, immune dysregulation, and microbial imbalance [5, 6]. These complexities complicate treatment because the underlying causative factors remain incompletely understood. Current therapies primarily focus on symptom management, including the use of emollients, glucocorticoids, antihistamines, immunosuppressants, biologics, and small-molecule inhibitors [7–9]. However, these conventional medications have limitations, such as unclear mechanisms of action, suboptimal bioavailability, potential side effects, and limited efficacy [10, 11]. Consequently, exploring safer and more effective treatment alternatives to address the unmet needs of patients with AD is imperative.

Mesenchymal stem cells (MSCs), which can be derived from various tissues, including the placenta, adipose tissue, bone marrow, and umbilical cord, exhibit potent paracrine and immunomodulatory properties [12, 13]. Furthermore, MSC therapy exhibits significant efficacy in preclinical models of inflammatory skin conditions, including AD, psoriasis, systemic scleroderma, systemic lupus erythematosus, and graft-versus-host disease [14–16]. Human umbilical cord mesenchymal stem cells (hUC-MSCs) offer several advantages, such as easy procurement, high purity, abundance, and enhanced activity. The use of hUC-MSCs circumvents the ethical concerns associated with stem cell research, minimizes immune rejection, and mitigates potential harm to donors and recipients. Allogeneic transplantation of hUC-MSCs elicits minimal immune responses and reduces tumorigenic risk without the use of immunosuppressants [17]. Although only a few studies have been carried out on hUC-MSC therapy for AD, current studies highlight its efficacy [18, 19]. These studies demonstrate that hUC-MSCs and their derivatives alleviate dermatitis symptoms and reduce the severity of skin lesions in animal models of AD [20]. hUC-MSCs also modulate inflammatory cytokines, including IgE, IL-6, IL-1β, and TNF-α, while increasing the expression of anti-inflammatory cytokines such as IL-10 and TGF-β1. A major clinical trial in South Korea investigated subcutaneous hUC-MSC implantation for AD treatment, yielding promising results [21]. Many patients experienced a decrease in the Eczema Area and Severity Index (EASI) and the Severity Score of Atopic Dermatitis (SCORAD), indicating the potential of hUC-MSCs for AD management. However, the therapeutic potential of hUC-MSC conditioned medium (hUC-MSC-CM), a cell-free alternative to hUC-MSCs, with lower tumorigenicity risk, remains largely underexplored. Moreover, mechanistic insights into neutrophil modulation and chemokine networks are lacking.

This study aimed to elucidate the mechanism of action of hUC-MSCs in AD treatment in a bit to advance our understanding of their therapeutic potential in the pathogenetic context of this disease. Sensitizer-induced AD mouse models, such as those established using ovalbumin (OVA) and 1-Chloro-2,4-dinitrobenzene (DNCB), are widely used in AD research due to their cost-effectiveness, simplicity, and high reproducibility. OVA induces allergic inflammation, while DNCB induces delayed-type hypersensitivity, both effectively inducing the inflammatory and pathological features of AD. In both mouse models, hUC-MSCs or hUC-MSC-CM was administered through subcutaneous injection, and the extent of skin damage, histological alterations, and changes in serum IgE levels were subsequently evaluated. Mechanistic investigations revealed that hUC-MSCs inhibited the JAK-STAT signaling pathway in keratinocytes via exosomal mechanisms, suppressed chemokine expression in these cells, and significantly reduced neutrophil infiltration in mouse skin, thereby exerting therapeutic effects.

Methods

Cell culture and treatment

hUC-MSCs and the cell diluents used in this study were prepared and supplied by S-Evans Biosciences Co., Ltd. (Hangzhou, China). hUC-MSCs at the fifth passage were selected for experimentation. Furthermore, as part of quality control, hUC-MSC surface marker expression was immunophenotyped via flow cytometry, as previously described [22]. Additionally, adipogenic and osteogenic differentiation assays were conducted to confirm hUC-MSC phenotypic identity. Human immortalized keratinocytes (HaCaT), obtained from Meisen CTCC (Zhejiang, China), were cultured in DMEM containing 10% fetal bovine serum and then incubated at 37 °C in a 5% CO_2 atmosphere.

hUC-MSC-CM and hUC-MSC-Exo preparation

The same batch of hUC-MSCs was diluted to a concentration of 2.0×10^5 cells/mL and cultured in

serum-free MSC culture medium. After 48 h, the resulting supernatant was collected and centrifuged at 3,000 rpm for 10 min to remove cells and debris, with the clarified supernatant retained. Then, hUC-MSC exosomes were extracted, and purified using an extracellular vesicle extraction kit (cell supernatant) (Umibio, Shanghai, China).

Murine AD model

For the DNCB-induced model, mice were randomly assigned to three groups (n = 6/group) i.e., the control group, the DNCB group, and either the DNCB + hUC-MSC or DNCB + hUC-MSCs-CM group in separate experiments. Mouse dorsal skin hair was shaved, and 200 μL of 1% DNCB (Sigma Aldrich, St. Louis, MO, USA) was applied to the skin. This treatment was repeated every two days for a total of four applications. Subsequently, 200 μL of 0.2% DNCB was applied following the same schedule for an additional four applications. On days 13, 17, 21, and 25, hUC-MSCs (2×10^6 cells/mL, 0.2 mL per administration) were administered by subcutaneous injection. Alternatively, hUC-MSCs-CM (0.4 mL per animal) was subcutaneously injected daily from day 10 for 14 consecutive days.

For the OVA-induced mouse model, all mice were randomly divided into three groups (n = 6/group) i.e., the control group, the OVA group, and either the OVA + hUC-MSC or OVA + hUC-MSCs-CM group in separate experiments. Mouse dorsal skin hair was shaved, and the skin barrier was disrupted by repeated application and removal of adhesive tape (8–10 times). Then, a sterile patch containing 1 μg/μL OVA (Sigma Aldrich St. Louis, MO, USA) was applied to the dorsal skin and replaced daily. From day 10, hUC-MSCs (2×10^6 cells/mL, 0.2 mL per administration) were subcutaneously injected into the patch-covered area every two days for a total of four injections. Alternatively, hUC-MSCs-CM (0.4 mL per animal) was subcutaneously injected daily from day 10 for 16 consecutive days.

During the experiment, no anesthesia was administered to the mice. Instead, all mice were euthanized by cervical dislocation. Subsequently, serum and skin samples were collected from the animals for further analysis. Blinding was not feasible during treatment; however, results were analyzed in a blinded manner whenever possible.

Cell proliferation assay

Cell proliferation was assessed following established protocols [23]. Briefly, HaCaT cells were exposed to various concentrations of Stattic (MCE, New Jersey, USA) for 48 h. After incubation, the cells were fixed with 10% (w/v) trichloroacetic acid and stained with sulforhodamine B (SRB) dye for 30 min. Subsequently, the SRB dye solution was dissolved using a 10 mM Tris-base alkali solution, and the absorbance was measured using a microplate reader.

Histopathological analyses

To evaluate skin thickening and immune cell infiltration, skin samples were collected, fixed in 10% formalin, and embedded in paraffin. Then, 5-μm-thick sections were prepared and subjected to dewaxing, hydration, hematoxylin dyeing, differentiation, eosin staining, and dehydration.

Real-time PCR

HaCaT cells were stimulated with TNF-α/IFN-γ (10 ng/mL; Sigma-Aldrich, MO, USA), hUC-MSC-CM (50%, v/v), hUC-MSC-Exos (20 μg/mL), or Stattic (10 μM) for 48 h. Overall, RNA was isolated using the TRIzol reagent (TaKaRa, Tokyo, Japan). cDNA was synthesized using the QuantiTect Reverse Transcription Kit (Qiagen, Hilden, Germany) according to the instructions of the manufacturer. qRT-PCR was performed using the SYBR Premix Ex Taq (Tli RNase H Plus; TaKaRa, Tokyo, Japan) on a CFX96 Touch Real-Time PCR Detection System (Bio-Rad, CA, USA). Table S1 lists the specific primer sequences used in this study. β-actin or Gapdh served as a reference gene, and the relative expression of target genes was calculated using the $2^{-\Delta\Delta Ct}$ method.

Western blotting

Tissue and cell samples were collected and lysed on ice using a lysis buffer. Proteins were extracted using the 1 × cell lysis buffer (Promega, USA), and then quantified using a BCA Protein Assay Kit (Pierce Biotechnology, Rockford, IL, USA). Proteins (20 μg) in each group were separated via 10% SDS-PAGE (Invitrogen, CA, USA) and then transferred onto PVDF membranes. Next, the membranes were blocked in TBST containing 5% skim milk and incubated overnight at 4 °C with primary antibodies, including anti-CD63 (Abcam, Cambridge, England), anti-TSG101, anti-STAT3, anti-P-STAT3, and anti-GAPDH (Proteintech, Wuhan, China) antibodies, all diluted at a 1:1000 ratio. After washing, the membranes were incubated with secondary antibodies (1:2000, Invitrogen, Carlsbad, CA, USA) at room temperature for 2 h. Finally, blots were visualized using an enhanced chemiluminescence (ECL) system (Beyotime, Nanjing, China).

Cytokine array

HaCaT cells were cultured in 6-well plates and exposed to TNF-α/IFN-γ (10 ng/mL) or hUC-MSC-CM (50%, v/v) for 48 h. The resulting supernatant from each group was collected, and chemokine expression levels in the

supernatant were determined using the Human Cytokine Array Kit (R&D Systems, Minneapolis, MN, USA) according to the instructions of the manufacturer.

Enzyme-linked immunosorbent assay (ELISA)

HaCaT cells were cultured in 6-well plates and exposed to TNF-α/IFN-γ (10 ng/mL) or hUC-MSCs-CM (50%, v/v) for 48 h. The culture medium was collected and centrifuged at 1000 g for 20 min. ELISA kits (Elabscience, Wuhan, China) were used to measure the concentrations of CCL5 and CXCL11 according to the instructions of the manufacturer.

Whole blood samples were collected from mice via orbital extraction. After allowing the blood to coagulate at room temperature for 30 min, the samples were centrifuged at 1000 g for 10 min at 4 ℃, and serum was collected. Serum IgE levels were determined using a mouse IgE enzyme-linked immunosorbent assay kit (Thermo Fisher, Pittsburgh, PA) according to the instructions of the manufacturer.

Flow cytometric analysis

Cells were isolated from the skin of BALB/c mice and resuspended in phosphate-buffered saline (PBS; Gibco, CA, USA) supplemented with 2% FBS. Then, the cells were incubated with TruStain fcX (anti-mouse CD16/32) antibodies (BioLegend, CA, USA) and stained with Pacific Blue anti-mouse CD45, APC anti-mouse CD11b, APC-Cyanine7 anti-mouse CD11c, PE anti-mouse F4/80, FITC anti-mouse Gr-1, APC-Cyanine7 anti-mouse Ly-6C, FITC anti-mouse Ly-6G, APC-Cyanine7 anti-mouse CD49b (pan-NK cells), APC anti-mouse CD3ε, BV510 anti-mouse CD4, and FITC anti-mouse CD8 antibodies. Before flow cytometric analysis, a 7-aminoactinomycin D (7-AAD) viability staining solution (BioLegend, San Diego, CA, USA) was added to the suspension to identify dead cells. Flow cytometry was conducted using a BD FACSCanto II device (BD Biosciences, USA), and data were analyzed using the FlowJo software.

RNA sequencing

RNA sequencing was outsourced to Hangzhou Lianchuan Biotechnology Co. Ltd. The general procedure was as follows: total RNA was extracted from HaCaT cells treated with or without TNF-α/IFN-γ (10 ng/mL; Sigma-Aldrich, MO, USA) for 48 h, and mRNA was isolated and purified. The RNA samples were converted into double-stranded cDNA. After filtering out low-quality sequences from the raw data using Cutadapt, valid data were obtained. Hisat2 was used for reference genome alignment. Based on the alignment results, Stringtie was used to reconstruct the transcripts and calculate the expression levels of all genes in each sample. Differentially expressed genes were identified using fold change threshold ≥ 2 and q value < 0.05 ($|\log2FC| \geq 1 \& q < 0.05$). The Lianchuan Biological Data Analysis Platform and the KEGG enrichment pathway analysis were used to evaluate the effects of the DEGs.

Transmission electron microscopy

Exosomes from hUC-MSCs were resuspended in 2% PFA. The vesicle suspension was applied onto a cover film, and a copper grid with a Formvar membrane facing downwards was placed on the suspension. Phosphate-buffered saline (PBS) was added to the cover film, and the copper grid was rinsed in the PBS droplet. Then, the grid was placed on 1% glutaraldehyde and rinsed eight times in ddH_2O. Subsequently, the copper grid was transferred to a uranyl acetate droplet at pH 7, and then to a methylcellulose droplet. Excess liquid on the copper grid was removed using filter paper, and the grid was air-dried before being placed in a storage box. Images were captured using a transmission electron microscope at 80 kV.

Nanoparticle tracking analysis (NTA)

Exosomes from hUC-MSCs were rinsed with deionized water. Next, a Particle Metrix nanoparticle tracking analyzer (ZetaView PMX 110) was calibrated with polystyrene microspheres (110 nm). After calibration, the sample cells were rinsed with 1 × PBS buffer (Biological Industries, Israel). Samples to be analyzed were diluted with 1 × PBS buffer (BI, Israel) before analysis.

Statistical analyses

Data are expressed as the mean ± standard error of the mean value (SEM) from at least three different experiments. T-tests and one-way or two-way analysis of variance (ANOVA) were performed using GraphPad Prism (GraphPad Software, California, USA) to evaluate the significance of the results. *P*-values < 0.05 were considered statistically significant.

Results

hUC-MSC treatment alleviates DNCB- and OVA-induced AD-like symptoms in mice

We investigated the therapeutic potential of subcutaneous hUC-MSC injection in a mouse model of DNCB-induced AD. hUC-MSCs significantly improved skin integrity in AD model mice by reducing skin symptoms, such as erythema, dryness, and crust formation, induced by DNCB (Fig. 1A). Hematoxylin and eosin (H&E) staining showed that hUC-MSC treatment decreased epidermal hyperplasia and inflammatory cell infiltration in AD model mouse skin (Fig. 1B). Additionally, hUC-MSC treatment increased the expression of levels of keratin

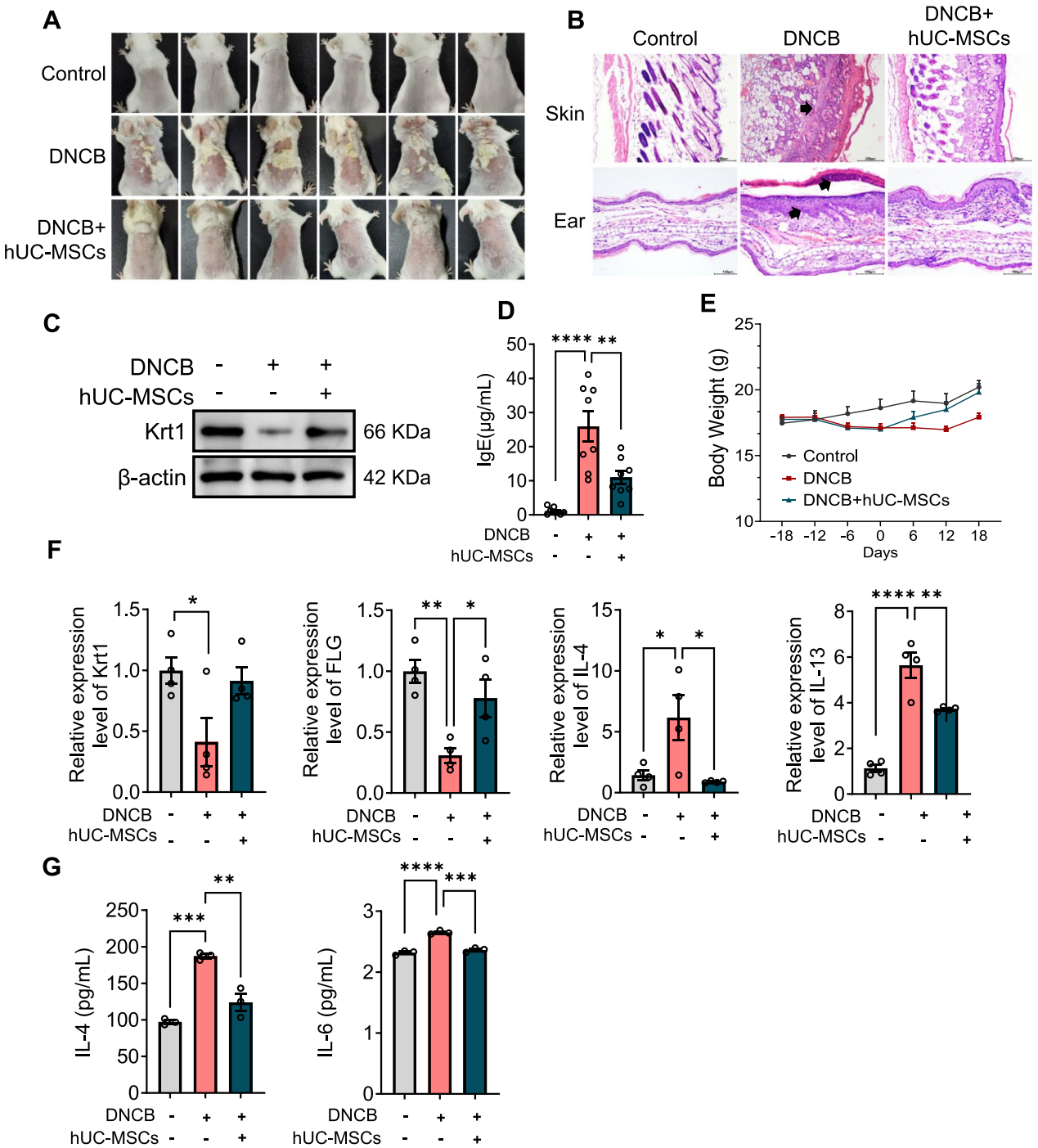

Fig. 1 hUC-MSC treatment improves DNCB-induced atopic dermatitis-like symptoms in mice. **A** Diagram showing damage of mouse dorsal skin following hUC-MSC treatment. **B** Representative H&E staining photomicrographs of mouse dorsal skin samples from the three groups; scale bar = 200 μm. **C** Western blot images showing Krt1 expression levels in mouse skin tissues. Full-length blots are presented in Supplementary Figure. **D** Changes in mouse IgE serum levels. **E** Changes in mouse body weight. **F** qRT-PCR analysis of FLG, Krt1, IL-4, and IL-13 mRNA expression in mouse skin tissues. **G** Changes in mouse serum IL-4 and IL-6 expression levels as detected through ELISA

1 (Krt1) and filaggrin (FLG), markers of skin barrier function (Fig. 1C and F). Moreover, as compared to the control treatment (the untreated AD model group), hUC-MSC treatment significantly decreased serum immunoglobulin E (IgE) levels, as well as the levels of key inflammatory markers and the cytokines, interleukin-4

(IL-4) and interleukin-6 (IL-6) (Fig. 1D, F, and G). These findings suggest that hUC-MSC treatment effectively alleviates DNCB-induced AD-like symptoms in mice. No weight loss was observed in mice following hUC-MSC treatment, suggesting the safety of this subcutaneous administration approach (Fig. 1E).

Similar results were obtained with the OVA-induced AD model, with hUC-MSC treatment effectively improving skin damage and reducing epidermal thickening and inflammatory cell infiltration (Fig. 2A and B). Immunohistochemical (IHC) analysis revealed that hUC-MSC treatment increased FLG protein levels and decreased serum IgE levels in OVA-induced model mice (Fig. 2C and D). Similarly, no weight loss was observed in OVA-induced model mice treated with hUC-MSCs (Fig. 2E).

hUC-MSC-CM treatment alleviates DNCB- and OVA-induced AD-like symptoms in mice

Studies have confirmed that the therapeutic effect of mesenchymal stem cells is predominantly mediated through the paracrine signaling pathway. Thus, we explored the therapeutic potential of hUC-MSC-CM. hUC-MSC-CM significantly mitigated skin damage (Fig. 3A and C), decreased epidermal thickening, and suppressed inflammatory cell infiltration (Fig. 3B and D) in DNCB- and OVA-induced AD models. Additionally, treatment with hUC-MSC-CM effectively reduced serum IgE levels (Fig. 3E). hUC-MSC-CM administration did not induce weight loss in mice in either model (Fig. 3F), underscoring its safety. Collectively, these findings demonstrate that hUC-MSC-CM treatment alleviates AD-like symptoms in DNCB- and OVA-induced AD mice. This suggests that the therapeutic effects of hUC-MSCs are mediated by their extracellular secretions via the paracrine pathway.

hUC-MSC-CM inhibits neutrophil migration in the skin

Immune dysregulation is a key mechanism and characteristic of AD. Both hUC-MSCs and hUC-MSC-CM decreased inflammatory cell infiltration in the skin tissues of AD model mice. Furthermore, we conducted a flow cytometric analysis on immune cells extracted from the dorsal skin and blood of DNCB-induced AD model mice (Supplementary Fig. 1). We found that there was a significant increase in the neutrophil population of the skin and blood, and that monocyte, macrophage, dendritic cell (DC), T cell,

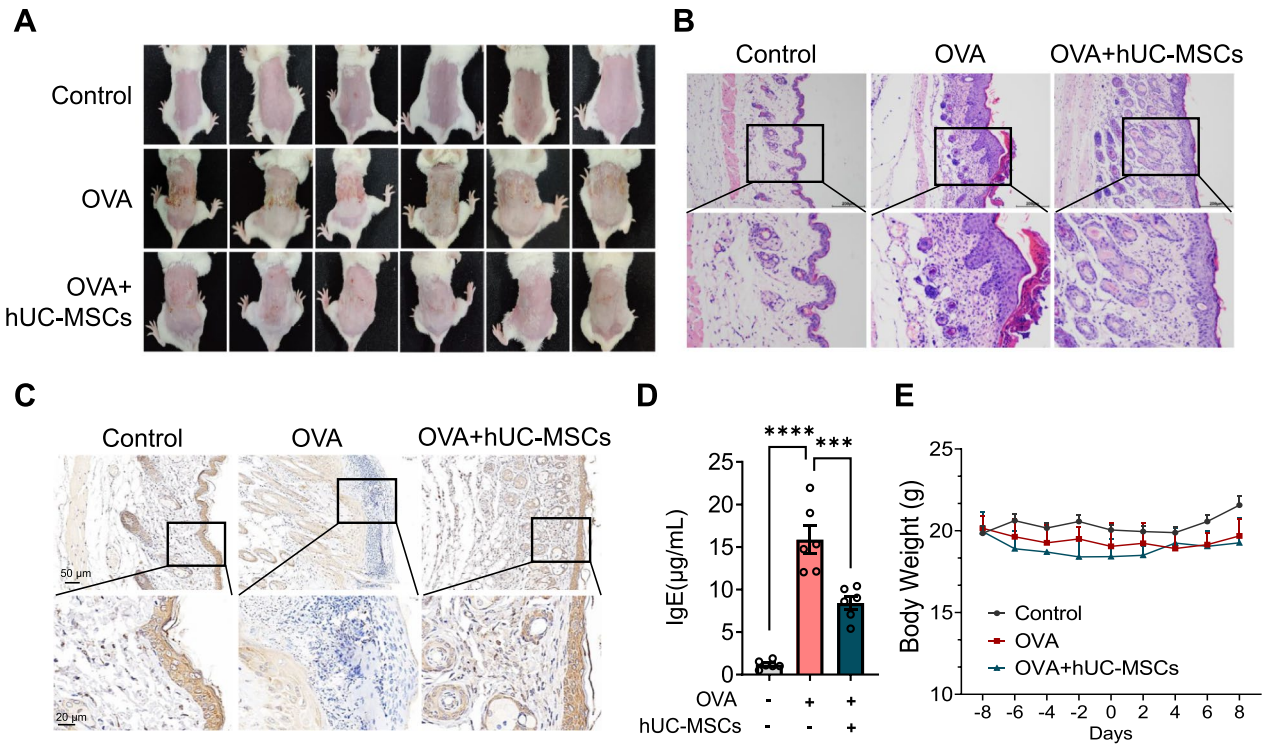

Fig. 2 hUC-MSC treatment improves atopic dermatitis-like symptoms in OVA-induced model mice. **A** Diagram showing damage of mouse dorsal skin following hUC-MSC treatment. **B** Representative H&E staining photomicrographs of mouse dorsal skin samples from the three groups; scale bar = 200 μm. **C** IHC analysis of FLG expression in mouse skin tissue; scale bar = 50 μm. **D** Changes in mouse IgE serum levels. **E** Changes in mouse body weight

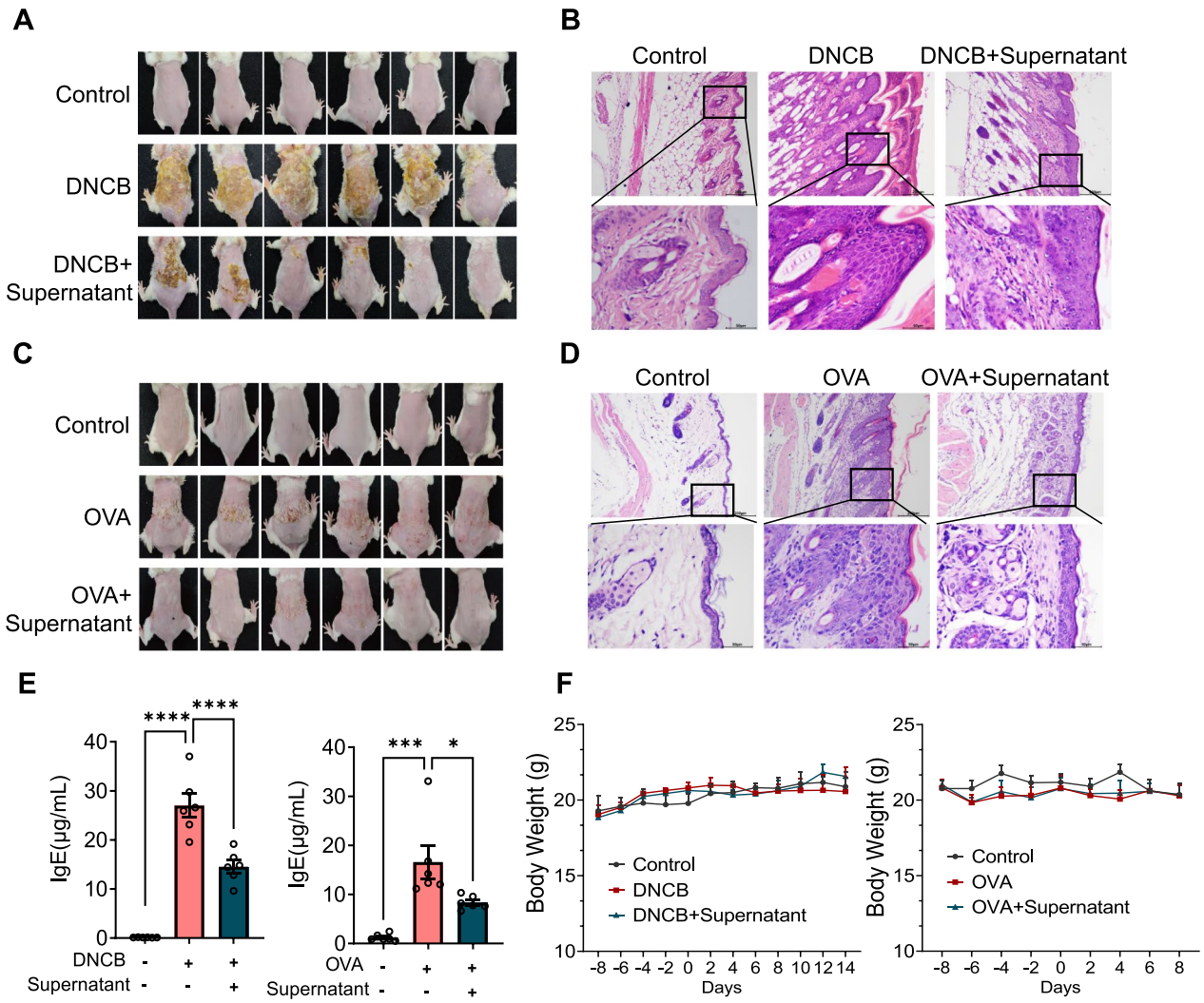

Fig. 3 Atopic dermatitis-like symptoms in DNCB- and OVA-induced BALB/c mice improve following hUC-MSC-CM treatment. **A** Changes in skin lesions on the backs of DNCB-induced mice after treatment with hUC-MSC-CM. **B** Representative H&E staining photomicrographs of dorsal skin samples from mice in the three groups following DNCB induction; scale bar = 200 μm. **C** Changes in DNCB-induced skin lesions on the backs of mice following hUC-MSC-CM treatment. **D** Representative H&E staining photomicrographs of dorsal skin samples from mice in the three groups following OVA induction. Scale bar = 200 μm. **E** Changes in mouse IgE serum levels following hUC-MSC-CM treatment. **F** Body weight changes in mice of the two model groups

and natural killer (NK) cell counts remained largely unchanged or decreased (Fig. 4A and B). Furthermore, hUC-MSC-CM inhibited the increase in neutrophil count, specifically within skin tissue (Fig. 4A), with minimal effects on blood neutrophil level (Fig. 4A). Consistent with these findings, immunofluorescence assays showed that hUC-MSC-CM significantly reduced neutrophil level in the skin (Fig. 4C). These findings collectively suggest that hUC-MSCs may exert therapeutic effects in AD by inhibiting neutrophil chemotaxis at sites of skin inflammation.

hUC-MSC-CM inhibits keratinocyte-derived chemokine secretion

Keratinocytes constitute the primary source of chemokines in the skin. To investigate this, we developed an in vitro AD model using the HaCaT keratinocyte cell line. RNA sequencing and KEGG pathway analyses were performed on RNA extracted from the control and AD model groups. We found significant activation of several cytokine-cytokine receptor interaction pathways in the AD model (Fig. 5A and B). Further analysis revealed an upregulation of chemokine expression in the model

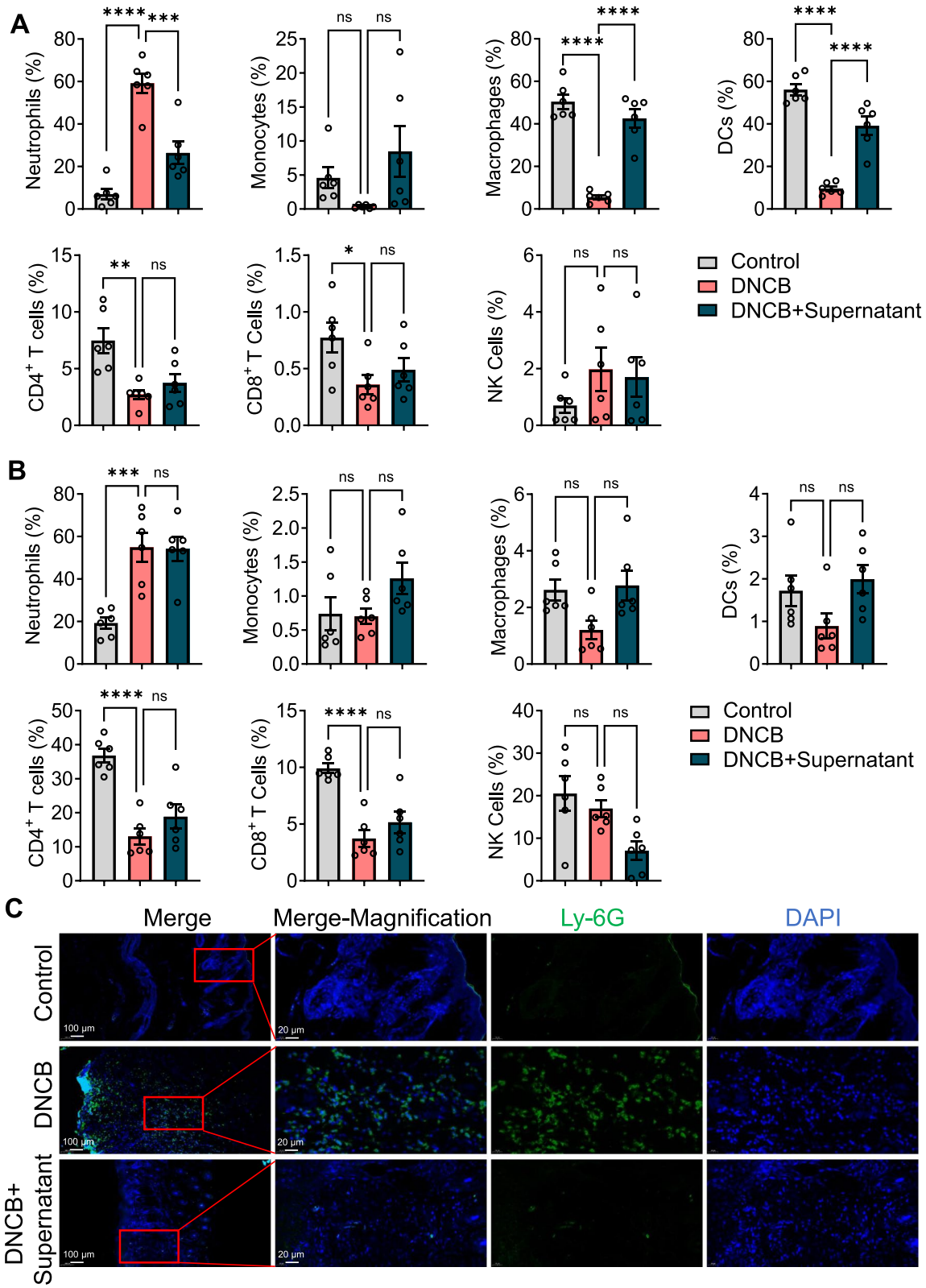

Fig. 4 hUC-MSC-CM inhibits neutrophil infiltration in mouse skin. **A** Changes in immune cell level in mouse skin and (**B**) blood as determined via flow cytometry. **C** Representative Ly-6G staining micrographs of dorsal skin samples from mice in the three groups as determined via immunofluorescence

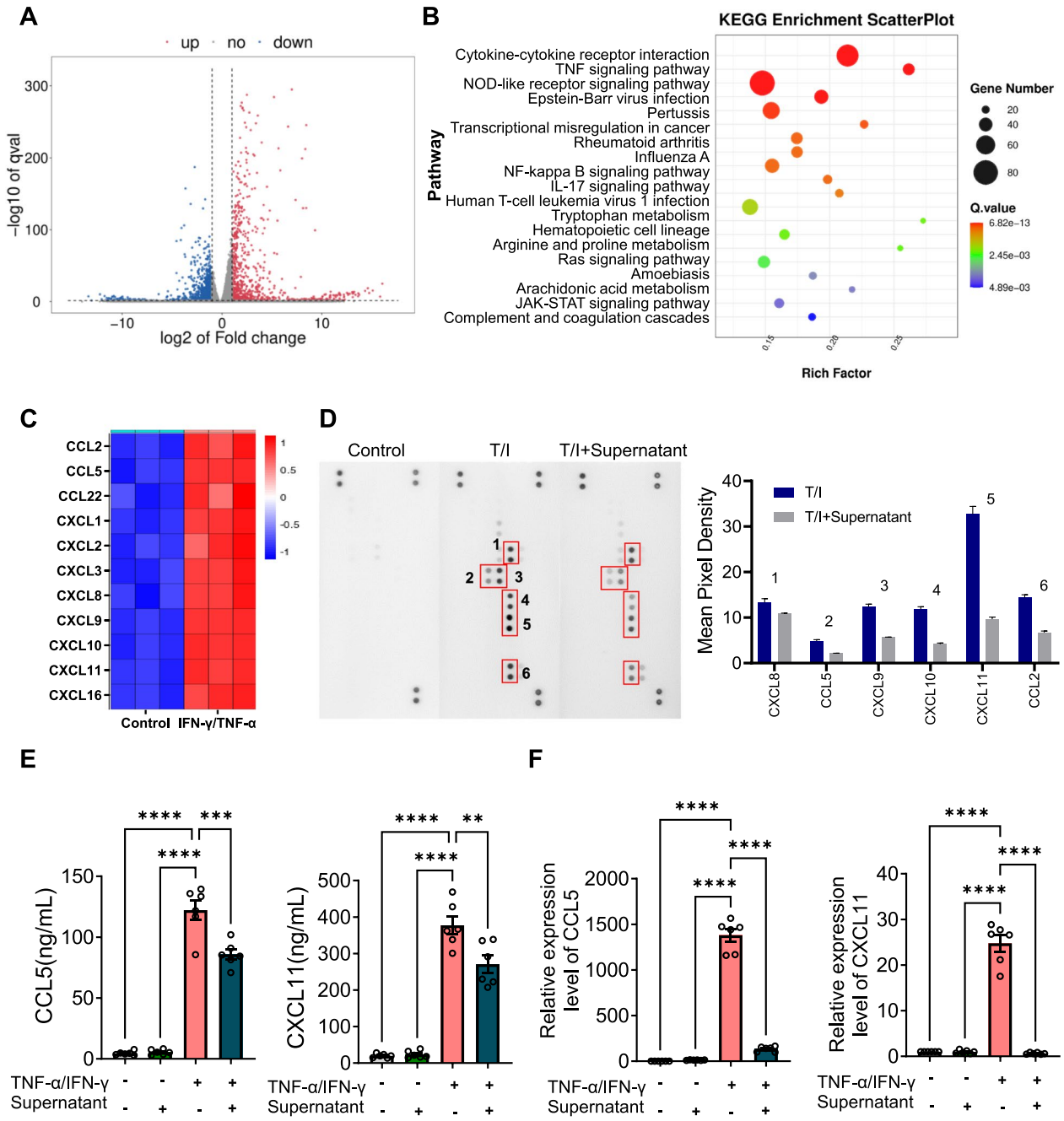

Fig. 5 hUC-MSC-CM inhibits keratinocyte-derived chemokine secretion. **A**–**C** HaCaT cells treated with TNF-α/IFN-γ (10 ng/mL) or left untreated for 48 h. **A** Volcano plot showing the differential mRNA expression profiles of HaCaT cells ($n = 3$ biological replicates). **B** KEGG analysis of signaling pathways upregulated in TNF-α/IFN-γ-treated HaCaT cells. **C** Changes in chemokine expression in HaCaT cells following TNF-α/IFN-γ treatment. **D**–**F** HaCaT cells were exposed to TNF-α/IFN-γ (T/I; 10 ng/mL) or hUC-MSC-CM (50%, v/v) for 48 h. **D** Chemokine array analysis of cell supernatants, with mean pixel density quantified using ImageJ. **E** ELISA images showing CCL5 and CXCL11 protein levels in the supernatants. **F** qRT-PCR analysis of CCL5 and CXCL11 mRNA expression in HaCaT cells

group (Fig. 5C). To confirm the regulatory effect of hUC-MSCs on chemokine expression, antibody arrays were performed for a more comprehensive analysis. Our experimental data showed elevated CCL2, CCL5, CXCL8, CXCL9, CXCL10, and CXCL11 protein levels in the AD model group, with hUC-MSC-CM effectively suppressing the expression of these chemokines (Fig. 5D). For additional validation, CCL5 and CXCL11 were

selected and their protein and mRNA levels assessed. ELISA and qPCR results showed a significant decrease in CCL5 and CXCL11 protein and mRNA levels following hUC-MSC-CM treatment (Fig. 5E and F). These findings collectively suggest that hUC-MSC-CM regulates chemokine activity, potentially representing a pivotal mechanism underlying its therapeutic efficacy against AD.

hUC-MSC-Exos inhibit chemokine production in keratinocytes

Exosomes are crucial paracrine effectors, recognized for their uniformity and diverse functions in cellular communication. To further ascertain the mechanisms underlying the effects of hUC-MSC-Exos against AD, purified exosomes were collected from hUC-MSC-CMs and isolated. Characterization of the exosomes—including their distribution, morphology, and marker expression—confirmed their successful isolation (Fig. 6A–C). In our in vitro AD model, co-culturing hUC-MSC-Exos with HaCaT keratinocytes led to significant inhibition of chemokine mRNA upregulation, particularly for CCL5 and CXCL11 mRNA, in the model group (Fig. 6D). This suggests that hUC-MSC-Exos regulate chemokine expression in keratinocytes through exosomal communication. This regulatory effect on chemokines may represent an important mechanism by which hUC-MSC-Exos contribute to AD inhibition.

The STAT3 signaling pathway mediates hUC-MSC-dependent chemokine regulation

The JAK-STAT signaling pathway plays a pivotal role in the pathophysiology of AD. KEGG pathway analysis showed a significant upregulation of the JAK-STAT signaling pathway in in vitro AD model TNF-α/IFN-γ treatment groups (Fig. 5B). Western blotting showed that hUC-MSCs decreased p-STAT3 protein levels in mouse skin tissue (Fig. 7A), and that exosomes reversed the TNF-α/IFN-γ-induced increase in p-STAT3 expression (Fig. 7B). To further evaluate the regulatory effect of the JAK-STAT signaling pathway on chemokine regulation, we assessed the effect of the STAT3 inhibitor, stattic, on chemokine expression in the in vitro AD model group. Initially, stattic exerted no significant effect on HaCaT cell viability (Fig. 7C). However, subsequently, it reversed the upregulation in chemokine mRNA

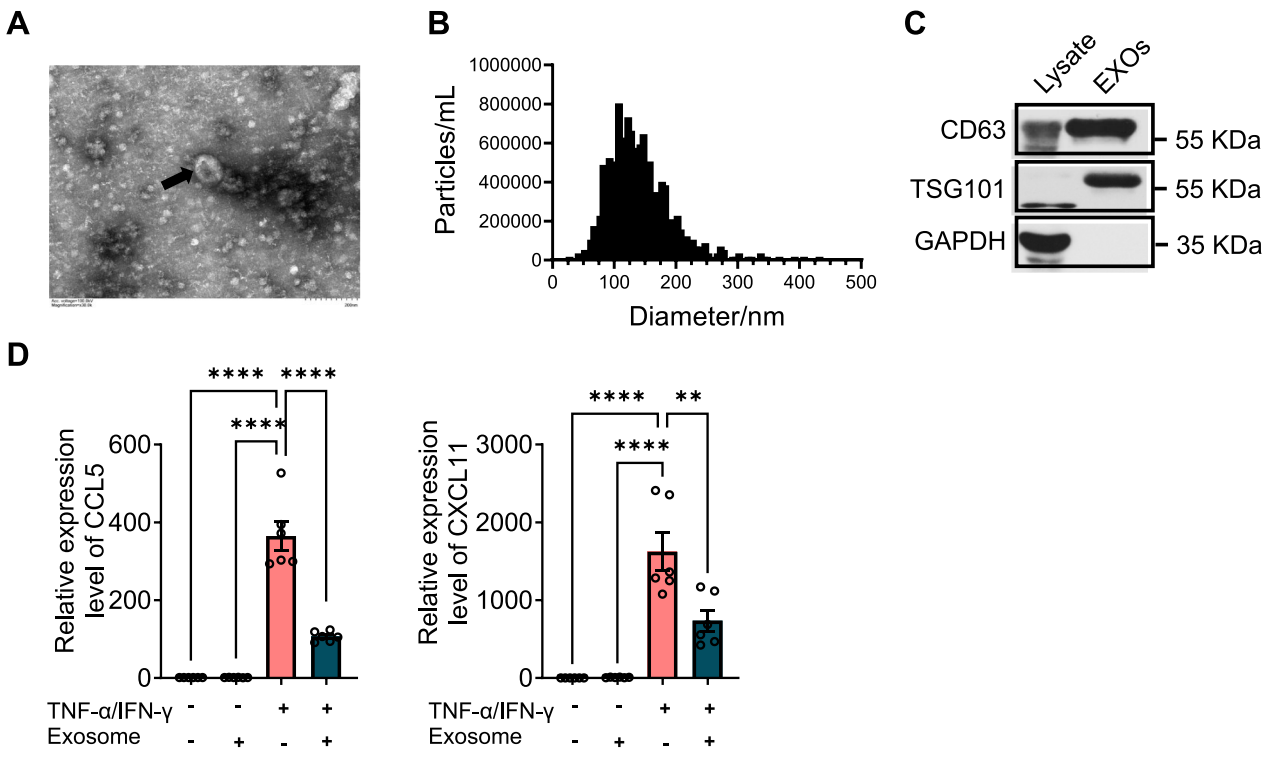

Fig. 6 hUC-MSC-Exos inhibit chemokine production in keratinocytes. **A** Images of hUC-MSC-Exos captured using a transmission electron microscope; black arrows indicate exosomes. **B** Nanoparticle tracking analysis using Particle Metrix reveals the size and concentration of hUC-MSC-Exos. **C** Western blot analysis of the exosome marker proteins, CD63 and TSG101. Full-length blots are presented in Supplementary Figure. **D** qRT-PCR analysis of chemokine mRNA expression in HaCaT cells treated with TNF-α/IFN-γ (10 ng/mL) or hUC-MSC-Exos (20 μg/mL) for 48 h

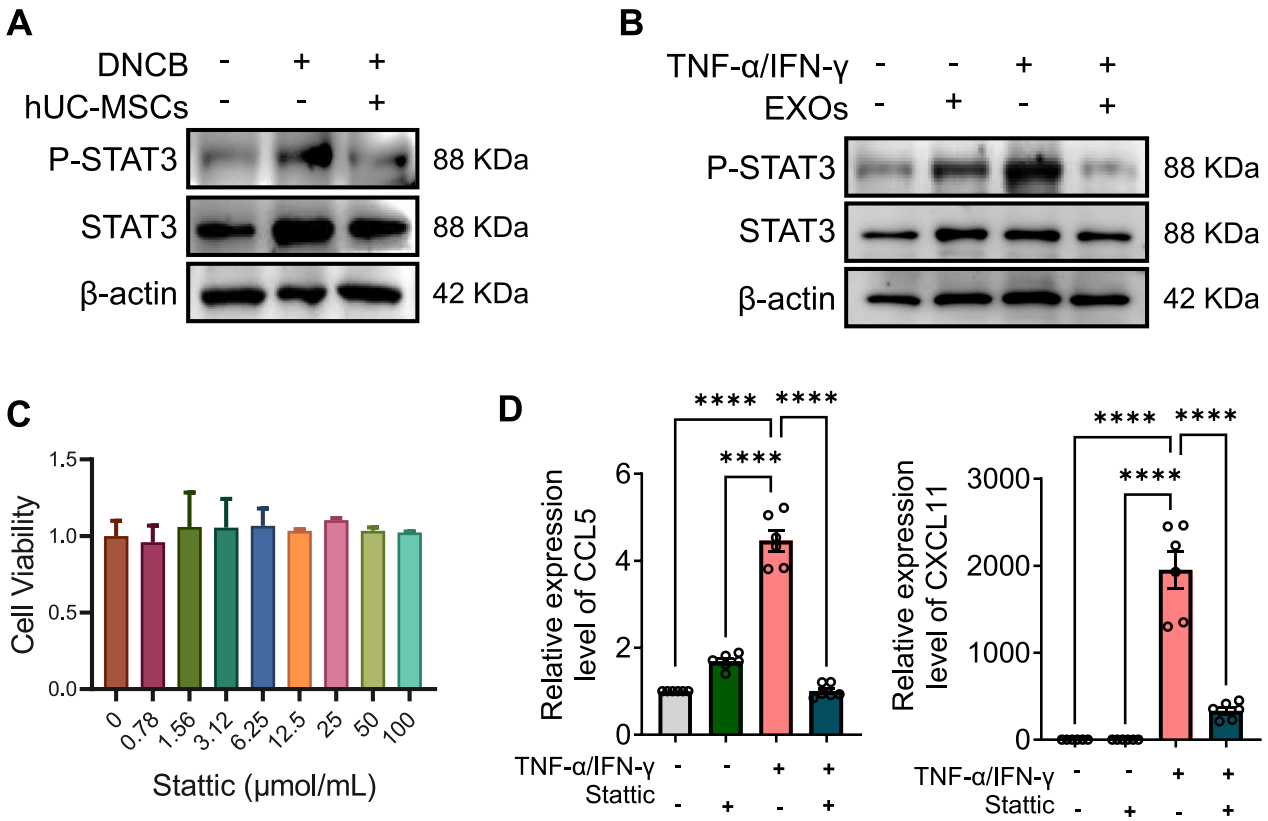

Fig. 7 The STAT3 signaling pathway mediates hUC-MSC-dependent chemokine regulation. **A** Changes in STAT3 signaling pathway activity in mouse skin following hUC-MSC treatment. **B** Western blot analysis of changes in STAT3 signaling pathway activity following treatment with exosomes. Full-length blots are presented in Supplementary Figure. **C** Effect of Stattic on HaCaT cell viability. **D** qRT-PCR analysis of HaCaT cell-related chemokine mRNA expression following treatment with Stattic (10 μM)

expression, particularly CCL5 and CXCL11 mRNA expression (Fig. 7D). These findings suggest that hUC-MSCs regulate chemokine expression via the JAK-STAT signaling pathway.

Discussion

Regenerative medicine has emerged as a promising field in dermatology, offering innovative therapeutic approaches for various skin conditions [24, 25]. Transplanted MSCs significantly improve organ function and modulate immunity through paracrine signaling pathways [26, 27]. Based on our confirmation that subcutaneous hUC-MSC injection ameliorates AD symptoms in OVA- and DNCB-induced AD models, we investigated whether hUC-MSC-CM exhibits similar therapeutic effects. Our findings indicated that hUC-MSC-CM effectively improves OVA- and DNCB-induced AD-like skin lesions and reduces serum IgE levels. Furthermore, we found that hUC-MSC-CM modulated the expression of chemokines in keratinocytes, thereby regulating neutrophil chemotaxis at dermatitis sites. Exosomes, key paracrine effectors, play a pivotal role in the effects of hUC-MSCs [28]. Extracellular vesicle subpopulations exhibit significant uniformity, diverse functions, and intricate compositions. hUC-MSC-derived exosomes were specifically evaluated in this study using an in vitro AD model. These exosomes effectively reduced chemokine production, suggesting that they could potentially replace hUC-MSCs or hUC-MSC-CM in AD treatment. In summary, hUC-MSCs hold promise as effective treatment agents for AD; however, further studies are needed to validate these findings.

Neutrophils are the most abundant circulating leukocytes in the body and the first immune cells to infiltrate the skin in patients with AD [29, 30]. They play a crucial role in mediating skin damage, itching, pain, and the inflammatory response in patients with AD [31, 32]. After production in the bone marrow through precursor cell differentiation, neutrophils rapidly migrate to damaged tissues and exert their effects during inflammatory injury [33]. Keratinocytes are the primary producers of chemokines in skin tissue; in acute AD models, they promote neutrophil infiltration in skin tissue by upregulating the secretion of chemokines,

such as CCL2 and CCL27 [34, 35]. Neutrophil-related chemokine expression is significantly high in patients with AD [30]. Blocking neutrophil chemotaxis using anti-CXCR2 antibodies effectively inhibits the inflammatory response [36]. Our findings suggests that hUC-MSCs may treat AD by inhibiting chemokine expression in keratinocytes and blocking neutrophil chemotaxis in skin tissue. Further investigations into the role and regulatory mechanisms of neutrophils in AD will potentially lead to breakthroughs in AD immunotherapy.

The JAK/STAT signaling pathway, which is frequently implicated in cytokine signal transduction, plays a key role in AD immune dysregulation [37]. It is involved in cell proliferation, differentiation, apoptosis, and inflammation, making it a potential target for AD treatment [38]. Currently, five JAK inhibitors have been approved globally for AD treatment; however, no STAT inhibitors have been identified [39]. Our results showed that hUC-MSCs and their exosomes could inhibit STAT3 expression, and that STAT inhibition may reduce chemokine expression in keratinocytes. These findings suggest that hUC-MSCs may inhibit the JAK/STAT signaling pathway in keratinocytes via exosomes, thereby inhibiting chemokine expression and neutrophil chemotaxis, and exerting a therapeutic effect against AD.

Conclusions

This study demonstrated that subcutaneous hUC-MSC and hUC-MSC-CM injection significantly improves AD-like skin symptoms. Further evaluation confirmed that it may inhibit chemokine expression in keratinocytes through exosomal regulation of the STAT3 signaling pathway, thereby blocking neutrophil chemotaxis and contributing to AD amelioration. Of note, hUC-MSC-CM was found to be a cell-free alternative for AD treatment, with comparable efficacy to whole-cell therapy, providing a promising translational strategy for AD treatment in clinical practice. These findings enhance our understanding of AD pathogenesis. In addition, our several comprehensive safety studies have been carried out on hUC-MSCs [18, 40–42], directly supporting the regulatory approval of a new drug clinical trial (IND) on "Human Umbilical Cord Mesenchymal Stem Cell Injection" (IND acceptance: CXSL2300670) for moderate-to-severe AD.

Abbreviations

AD	Atopic dermatitis
ANOVA	Analysis of variance
DC	Dendritic cell
DNCB	1-Chloro-2,4-dinitrobenzene
ECL	Enhanced chemiluminescence
FLG	Filaggrin
HaCaT	Human immortalized keratinocytes
hUC-MSCs	Human umbilical cord mesenchymal stem cells
hUC-MSC-CM	Human umbilical cord mesenchymal stem cell conditioned medium
IgE	Immunoglobulin E
IHC	Immunohistochemistry
IL	Interleukin
Krt1	Keratin 1
MSCs	Mesenchymal stem cells
NK	Natural killer
NTA	Nanoparticle tracking analysis
OVA	Ovalbumin
PBS	Phosphate-buffered saline
SEM	Standard error of the mean
SRB	Sulforhodamine B

Supplementary Information

The online version contains supplementary material available at https://doi.org/10.1186/s13287-025-04349-8.

Additional file 1.

Acknowledgements

The authors declare that they have not used AI-generated work in this manuscript.

Author contributions

LZ, JL, and RP conceptualized the study; JS, ZX, ZY, GC, and LZ developed the methodology and experimental design; SJ, ZX, ZY, GC, YW, XL, LZ, LZ, FL, and SZ conducted the investigation and experiments; ZY, GC, YW, LZ, FL, SZ, XL, RP, and FW validated the experiment; JS and ZX performed formal data analysis; JS and ZX wrote the original draft; YC, YC, LZ, and JZ reviewed and edited the manuscript; JS and ZX visualized the data and prepared the figures; LZ, JL, and RP supervised the study. All the authors have reviewed the manuscript and provided comments.

Funding

This study was funded by the Key R&D Program of Zhejiang Province (grant no. 2021C03077) and the National Natural Science Foundation of China (grant no. 82404122).

Availability of data and materials

The sequencing datasets supporting this study are publicly accessible in the NCBI GEO repository under accession number, GSE277914. All additional experimental data and analytical results are available within the manuscript and its supplementary files. Additional details can be obtained from the corresponding authors upon reasonable request.

Declarations

Ethics approval and consent to participate

Female 5–7-week-old BALB/c mice were obtained from the Experimental Animal Center of Hangzhou Medical College and Zhejiang Vital River Laboratory Animal Technology (Zhejiang, China). The mice were housed in barrier facilities under specific pathogen-free conditions and maintained under a 12-h light/dark cycle, with unrestricted access to food and water. The animal study protocol was approved by the Institutional Animal Care and Use Committee (IACUC) of Hangzhou Medical College under the project titled, "Research on Novel Diagnostic and Therapeutic Techniques for Dermatological, Venereological, and Rheumatological Immune Diseases-Development of Umbilical Cord Mesenchymal Stem Cell-Based Therapy for Atopic Dermatitis" (Approval No: 2024–033; Date of Approval: April 11, 2024). The animal study has been reported according to ARRIVE 2.0 guidelines. The hUC-MSCs used in this study were provided for research purposes by S-Evans Biosciences. The supplier confirmed that original umbilical cord tissue collection was conducted following the protocol, "Collection, Preparation, and Preservation of Umbilical Cord and Placental Stem Cells," approved by the Ethics Committee for Human Research at the Second Affiliated Hospital of Zhejiang University School of Medicine (Approval No. 2021–1135; Date of Approval: December 24, 2021); in addition, they confirmed that informed consent was obtained from all donors prior to tissue collection. As this study

was conducted on pre-collected, anonymized cells, and did not involve direct human participation, no additional ethics approval was required for their use.

Consent for publication
Not applicable.

Competing interests
The authors declare that they have no competing interests.

Author details
[1]Key Laboratory of Drug Safety Evaluation and Research of Zhejiang Province, Center of Safety Evaluation and Research, Hangzhou Medical College, Hangzhou 310053, China. [2]Wuyi First People's Hospital, Affiliated Hospital, School of Medicine, Hangzhou City University, Hangzhou 310015, China. [3]Zhejiang Key Laboratory of Cell-Based Drug and Applied Technology Development, S-Evans Biosciences Co., Ltd., Hangzhou, China. [4]Zhejiang Center for Drugs and Cosmetics Evaluation, Zhejiang Province Food and Drug Administration, Hangzhou 310012, China. [5]Faculty of Chinese Medicine, Macau University of Science and Technology, Macao 999078, China. [6]Qingshan Lake Science and Technology Innovation Center, Hangzhou Medical College, Hangzhou 311306, China.

Received: 3 February 2025 Accepted: 17 April 2025
Published online: 14 May 2025

References

1. Bieber T. Atopic dermatitis: an expanding therapeutic pipeline for a complex disease. Nat Rev Drug Discov. 2022;21:21–40.
2. Stander S. Atopic dermatitis. N Engl J Med. 2021;384:1136–43.
3. Guttman-Yassky E, Renert-Yuval Y, Brunner PM. Atopic dermatitis. Lancet. 2025;405:583–96.
4. Langan SM, Irvine AD, Weidinger S. Atopic dermatitis. Lancet. 2020;396:345–60.
5. Sroka-Tomaszewska J, Trzeciak M. Molecular mechanisms of atopic dermatitis pathogenesis. Int J Mol Sci. 2021;22:4130.
6. Facheris P, Jeffery J, Del Duca E, Guttman-Yassky E. The translational revolution in atopic dermatitis: the paradigm shift from pathogenesis to treatment. Cell Mol Immunol. 2023;20:448–74.
7. Li H, Zhang Z, Zhang H, Guo Y, Yao Z. Update on the pathogenesis and therapy of atopic dermatitis. Clin Rev Allergy Immunol. 2021;61:324–38.
8. Freitas E, Gooderham M, Torres T. New topical therapies in development for atopic dermatitis. Drugs. 2022;82:843–53.
9. Newsom M, Bashyam AM, Balogh EA, Feldman SR, Strowd LC. New and emerging systemic treatments for atopic dermatitis. Drugs. 2020;80:1041–52.
10. Chovatiya R, Paller AS. JAK inhibitors in the treatment of atopic dermatitis. J Allergy Clin Immunol. 2021;148:927–40.
11. Bieber T. Disease modification in inflammatory skin disorders: opportunities and challenges. Nat Rev Drug Discov. 2023;22:662–80.
12. Jiang W, Xu J. Immune modulation by mesenchymal stem cells. Cell Prolif. 2020;53: e12712.
13. Wang Y, Fang J, Liu B, Shao C, Shi Y. Reciprocal regulation of mesenchymal stem cells and immune responses. Cell Stem Cell. 2022;29:1515–30.
14. Yang J, Xiao M, Ma K, Li H, Ran M, Yang S, et al. Therapeutic effects of mesenchymal stem cells and their derivatives in common skin inflammatory diseases: atopic dermatitis and psoriasis. Front Immunol. 2023;14:1092668.
15. Veglia F, Sanseviero E, Gabrilovich DI. Myeloid-derived suppressor cells in the era of increasing myeloid cell diversity. Nat Rev Immunol. 2021;21:485–98.
16. Al-Masawa ME, Elfawy LA, Ng CY, Ng MH, Law JX. Mesenchymal stromal cell-derived extracellular vesicles in the management of atopic dermatitis: a scoping review of therapeutic opportunities and challenges. Int J Nanomedicine. 2025;20:2673–93.
17. Xie Q, Liu R, Jiang J, Peng J, Yang C, Zhang W, et al. What is the impact of human umbilical cord mesenchymal stem cell transplantation on clinical treatment? Stem Cell Res Ther. 2020;11:519.
18. Hua C, Liang Q, Chen S, Zhu J, Tang Y, Chen X, et al. Human umbilical cord mesenchymal stem cell treatment alleviates symptoms in an atopic dermatitis-like mouse model. Stem Cell Res Ther. 2023;14:147.
19. Song JY, Kang HJ, Ju HM, Park A, Park H, Hong JS, et al. Umbilical cord-derived mesenchymal stem cell extracts ameliorate atopic dermatitis in mice by reducing the T cell responses. Sci Rep. 2019;9:6623.
20. Najera J, Hao J. Recent advance in mesenchymal stem cells therapy for atopic dermatitis. J Cell Biochem. 2023;124:181–7.
21. Kim HS, Lee JH, Roh KH, Jun HJ, Kang KS, Kim TY. Clinical trial of human umbilical cord blood-derived stem cells for the treatment of moderate-to-severe atopic dermatitis: Phase I/IIa studies. Stem Cells. 2017;35:248–55.
22. Liu F, Song DY, Huang J, Yang HQ, You D, Ni JD. Long non-coding RNA CIR inhibits chondrogenic differentiation of mesenchymal stem cells by epigenetically suppressing ATOH8 via methyltransferase EZH2. Mol Med. 2021;27:12.
23. Xu L, Zhu Y, Shao J, Chen M, Yan H, Li G, et al. Dasatinib synergises with irinotecan to suppress hepatocellular carcinoma via inhibiting the protein synthesis of PLK1. Br J Cancer. 2017;116:1027–36.
24. Jafarzadeh A, Pour Mohammad A, Keramati H, Zeinali R, Khosravi M, Goodarzi A. Regenerative medicine in the treatment of specific dermatologic disorders: a systematic review of randomized controlled clinical trials. Stem Cell Res Ther. 2024;15:176.
25. Jafarzadeh A, Mohammad AP, Goodarzi A. A systematic review of case series and clinical trials investigating regenerative medicine for the treatment of vitiligo. J Cosmet Dermatol. 2025;24: e16660.
26. Shen Z, Huang W, Liu J, Tian J, Wang S, Rui K. Effects of mesenchymal stem cell-derived exosomes on autoimmune diseases. Front Immunol. 2021;12: 749192.
27. Zheng Q, Zhang S, Guo WZ, Li XK. The unique immunomodulatory properties of MSC-derived exosomes in organ transplantation. Front Immunol. 2021;12: 659621.
28. Kalluri R, LeBleu VS. The biology, function, and biomedical applications of exosomes. Science. 2020. https://doi.org/10.1126/science.aau6977.
29. Phillipson M, Kubes P. The healing power of neutrophils. Trends Immunol. 2019;40:635–47.
30. Choy DF, Hsu DK, Seshasayee D, Fung MA, Modrusan Z, Martin F, et al. Comparative transcriptomic analyses of atopic dermatitis and psoriasis reveal shared neutrophilic inflammation. J Allergy Clin Immunol. 2012;130:1335-43.e5.
31. Pavlenko D, Todurga Seven Z, Bystrom L, Markan A, Verpile R, Ishida H, et al. Crisaborole inhibits itch and pain by preventing neutrophil infiltration in a mouse model of atopic dermatitis. Acta Derm Venereol. 2023. https://doi.org/10.2340/actadv.v103.13382.
32. Walsh CM, Hill RZ, Schwendinger-Schreck J, Deguine J, Brock EC, Kucirek N, et al. Neutrophils promote CXCR3-dependent itch in the development of atopic dermatitis. Elife. 2019;8: e48448.
33. Özcan A, Boyman O. Mechanisms regulating neutrophil responses in immunity, allergy, and autoimmunity. Allergy. 2022;77:3567–83.
34. Das P, Mounika P, Yellurkar ML, Prasanna VS, Sarkar S, Velayutham R, et al. Keratinocytes: an enigmatic factor in atopic dermatitis. Cells. 2022;11:1683.
35. Chieosilapatham P, Kiatsurayanon C, Umehara Y, Trujillo-Paez JV, Peng G, Yue H, et al. Keratinocytes: innate immune cells in atopic dermatitis. Clin Exp Immunol. 2021;204:296–309.
36. Alam MJ, Xie L, Ang C, Fahimi F, Willingham SB, Kueh AJ, et al. Therapeutic blockade of CXCR2 rapidly clears inflammation in arthritis and atopic dermatitis models: demonstration with surrogate and humanized antibodies. MAbs. 2020;12:1856460.
37. Huang IH, Chung WH, Wu PC, Chen CB. JAK-STAT signaling pathway in the pathogenesis of atopic dermatitis: an updated review. Front Immunol. 2022;13:1068260.
38. Tsiogka A, Kyriazopoulou M, Kontochristopoulos G, Nicolaidou E, Stratigos A, Rigopoulos D, et al. The JAK/STAT pathway and its selective inhibition in the treatment of atopic dermatitis: A systematic review. J Clin Med. 2022;11:4431.
39. Tsuji G, Yamamura K, Kawamura K, Kido-Nakahara M, Ito T, Nakahara T. Novel therapeutic targets for the treatment of atopic dermatitis. Biomedicines. 2023;11:1303.

40. Xia L, Shao J, Yang Q, Zhang C, Xie Z, Wang L, et al. Repeat-dose toxicity of human umbilical cord mesenchymal stem cells via subcutaneous injection in NOG mice. Front Cell Dev Biol. 2025;13:1558310.
41. Shao J, Xia L, Ye Z, Yang Q, Zhang C, Shi Y, et al. A repeat-dose toxicity study of human umbilical cord mesenchymal stem cells in NOG mice by intravenous injection. Expert Opin Drug Metab Toxicol. 2023;19:857–66.
42. Pan W, Gu L, Yang H, Xu C, Yang Z, Lu Q, et al. Repeat-dose toxicity study of human umbilical cord mesenchymal stem cells in cynomolgus monkeys by intravenous and subcutaneous injection. Front Cell Dev Biol. 2023;11:1273723.

Publisher's Note